Localization noise in deep subwavelength plasmonic devices

Ali Ghoreyshi[1] and R. H. Victora[1,2,*]

[1]*Department of Electrical and Computer Engineering, University of Minnesota, Minneapolis, Minnesota 55455, USA*

[2]*School of Physics and Astronomy, University of Minnesota, Minneapolis, Minnesota 55455, USA*

(Received 17 November 2017; revised manuscript received 13 March 2018; published 17 May 2018)

The grain shape dependence of absorption has been investigated in metal-insulator thin films. We demonstrate that randomness in the size and shape of plasmonic particles can lead to Anderson localization of polarization modes in the deep subwavelength regime. These localized modes can contribute to significant variation in the local field. In the case of plasmonic nanodevices, the effects of the localized modes have been investigated by mapping an electrostatic Hamiltonian onto the Anderson Hamiltonian in the presence of a random vector potential. We show that local behavior of the optical beam can be understood in terms of the weighted local density of the localized modes of the depolarization field. Optical nanodevices that operate on a length scale with high variation in the density of states of localized modes will experience a previously unidentified localized noise. This localization noise contributes uncertainty to the output of plasmonic nanodevices and limits their scalability. In particular, the resulting impact on heat-assisted magnetic recording is discussed.

DOI: 10.1103/PhysRevB.97.205430

Anderson localization of light has attracted extensive attention from both application and theoretical perspectives during the past decade [1–6]. In this context, existence of strong disorder can prohibit propagation of the light owing to constructive interference of scattered waves at their point of origin. Being an interference effect, adequate phase accumulation between scattering events is essential for complete localization. Using plasmonic materials, this phenomenon has been investigated in various structures [7–9]. However, there is no indication that Anderson localization is a significant phenomenon when separation between plasmonic scatterers is much smaller than the wavelength ($d \approx \lambda/1000$).

In this paper, on the other hand, we demonstrate that, in an ensemble of plasmonic particles, randomness in shape, size, or position of particles can lead to Anderson localization of light in the near-field regime, even though the distance between particles is much shorter than the wavelength. This phenomenon can be understood from the perspective of photons hopping between plasmonic particles. From this point of view, the large negative value of the real part of plasmonic particles' permittivity, separated by a dielectric, binds photons to the particle [10–14]; however, they can hop between them through the dipole-dipole interaction. In such systems, randomness in the optical properties of particles can act similarly to the random potential in the Anderson Hamiltonian (AH) and lead to localization of photons.

Although these localized modes can be beneficial for various applications [15–17], we study them in the context of the uncertainty that they bring to the local-field behavior and restrictions to the scalability of plasmonic devices, which we denote as localization noise. In order to quantify the behavior of the localization noise, we first study the effects of shape and permittivity on the depolarization field of an isolated particle. Then, we investigate Anderson localization due to dipole-dipole interactions in a random ensemble of plasmonic particles. Finally, by mapping an electrostatic Hamiltonian onto the Anderson Hamiltonian in the presence of a random vector potential [18–20], we demonstrate that the localization noise is an explicit consequence of variation in the local density of states of the localized plasmonic modes. To provide a context for our results, we investigate the influence of the localized noise on heat-assisted magnetic recording (HAMR) [21–23], which operates in the smallest regime feasible for a plasmonic device.

The total electric field inside ponderable materials can be written as a superposition of applied E_0 and the depolarization field E_d of the induced dipole moment ($E = E_0 + E_d$). For a linear isotropic particle located in vacuum, the electric field inside the particle can be written as

$$|E|^2 = |E_0|^2 \sum_{i=x,y,z} \left| \frac{1}{1 + N_{ii}(\epsilon_r - 1)} \right|^2, \qquad (1)$$

where E_0 is the projection of the applied field on the x, y, and z axes, ϵ_r is the permittivity of the particle, and N_{ii} is the depolarization factor along different directions ($i = x,y,z$) [24].

Without loss of generality, we can assume that the shape of the particle represents deformation from a sphere ($N_{xx} = N_{yy} = N_{zz} = 1/3$) such that $N_{xx} + N_{yy} = 2/3$ and $N_{zz} = 1/3$. By applying the external field on the x-y plane, two resonances can be observed corresponding to two different values of N_{xx} [Fig. 1(a)]. Depending on the permittivity of the particle, these resonances can happen inside or outside the acceptable range of $N_{xx}(0 \leqslant N_{xx} \leqslant 2/3)$. For $\epsilon_r > 0$, resonances correspond to unacceptable values of N_{xx} ($N_{xx} < 0$ and $N_{xx} > 2/3$). However, for the case of $\epsilon_r < 0$, resonances happen at the acceptable values of N_{xx}, and the electric field can be enhanced inside the particle. This is the reason for extraordinary local-field enhancement in low loss plasmonic particles,

*victora@umn.edu

 ©2018 American Physical Society

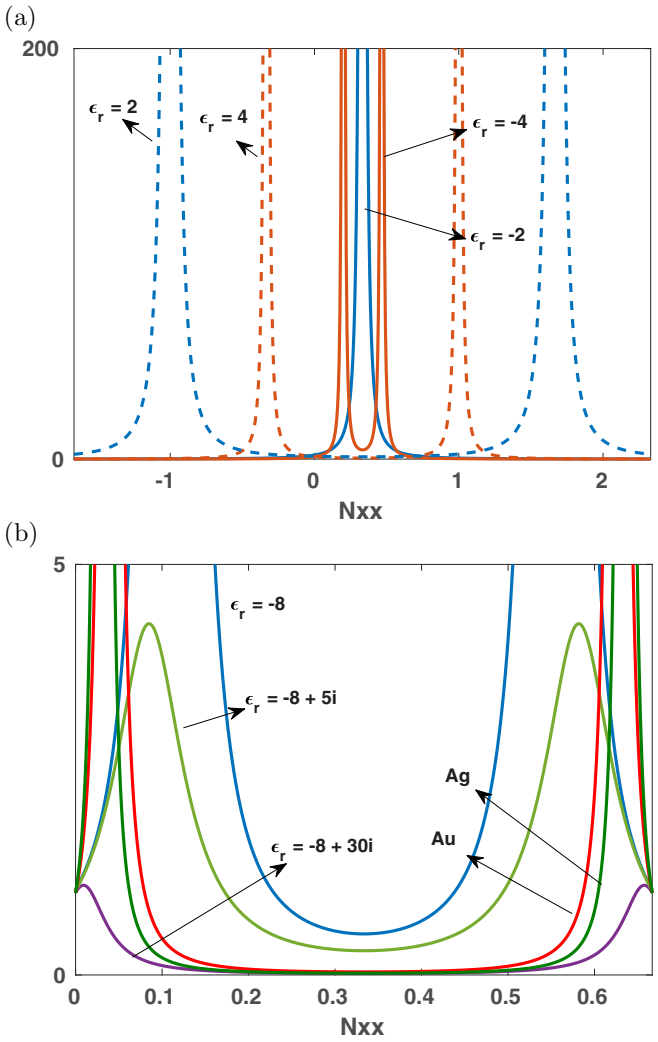

FIG. 1. (a) Total field intensity inside an isolated particle for different values of permittivity as a function of depolarization factor and (b) the effect of the material loss on the field enhancement inside the particle. Permittivity of Au and Ag is evaluated at $\lambda = 800$ nm.

such as Au and Ag. In the case of lossy metallic particles, on the other hand, these resonances are not significant, and most of the energy is damped as heat inside the particles. As demonstrated in Fig. 1(b), the peak value of the electric field decreases as $\mathrm{Im}\{\epsilon_r\}$ increases. However, from the local-field fluctuation perspective, any sort of randomness in the shape of the particle, even for the case of lossy materials, can drastically affect the optical response of the particles.

In order to investigate the localization in a system of randomly distributed plasmonic particles, we use an analogous method to the discrete dipole approximation (DDA) method [25] and write the induced dipole moment for a particle located at r_i as

$$p_i = \alpha_i E_{\mathrm{loc}}(r_i), \tag{2}$$

where α is the polarizability and E_{loc} is the sum of an incident field and the contributed field from all other particles,

$$E_{\mathrm{loc}}(r_i) = E_0(r_i) + \sum_{i \neq j} A_{ij} p_j, \tag{3}$$

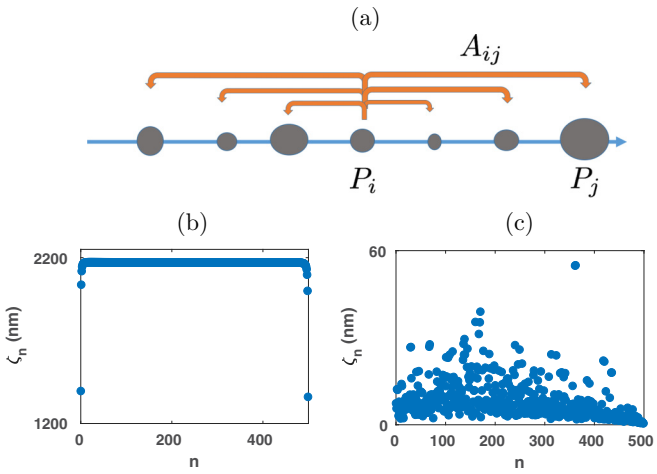

FIG. 2. (a) Schematic of a random array of plasmonic particles with long-range interaction between them, (b) localization length of an array of particles ($\epsilon_r = -1$) with constant separation distance, and (c) localization length for an array of randomly located particles ($\epsilon_r = -1$).

where A_{ij} is the dipole-dipole interaction matrix and can be written as [26]

$$A_{ij} = \frac{e^{ikr_{ij}}}{|r_{ij}|}\left[k^2\left(\mathbf{I}_{3\times3} - \frac{\mathbf{r}_{ij}\otimes\mathbf{r}_{ij}}{|r_{ij}|^2}\right) - \frac{1-ik|r_{ij}|}{|r_{ij}|^2}\left(\mathbf{I}_{3\times3} - 3\frac{\mathbf{r}_{ij}\otimes\mathbf{r}_{ij}}{|r_{ij}|^2}\right)\right]. \tag{4}$$

For the deep subwavelength regime, the retardation of the electromagnetic wave can be ignored, and the contribution from the other particles can be obtained from Eq. (4) by $kr \longrightarrow 0$. Therefore, Eq. (3) can be considered as

$$S|p\rangle = |E_0\rangle, \tag{5}$$

where all the interactions between the particles are included in the tensor S and polarization modes of the system can be described in terms of eigenvectors of S. In order to investigate the effects of randomness on the collective response of the particles, we calculate localization lengths of polarization modes in a one-dimensional (1D) array of 500 spherical plasmonic particles with a radius of 5 nm ($\epsilon_r = -1$) with 15-nm separation for two cases: The radii of the particles are constant, and a 20% variation is added to the particles [Fig. 2(a)]. The separation between the particles has been selected to be large enough ($D/2R \approx 1.5$) to meet the accuracy criteria of the DDA method ($D/2R > 1.25$) [27,28]. For each case, we calculate the localization length of the eigenstates of S using

$$\zeta_n^2 = \int (r - \langle r\rangle_n)^2 |\psi_n|^2 dr, \tag{6}$$

where ψ_n is the nth eigenstate of S and $\langle r\rangle_n = \int r|\psi_n|^2 dr$. As depicted in Fig. 2, for the case of constant distance between the particles, the eigenstates are extended through the particle array. On the other hand, adding randomness to the location of the particles leads to localization of all the eigenstates. Similar

behavior is observed for other types of randomness, such as random size or shape.

These results can be understood more clearly by comparing tensor S with the Anderson Hamiltonian: Randomness in polarizability of individual particles can be interpreted as on-diagonal random energy matrix elements in the Anderson model, whereas the off-diagonal elements can be considered as the hopping probability. From this perspective, the randomness in plasmonic properties of different particles behaves similarly to the random potential in the Anderson model. In such systems, there is no length scale limit due to interference, and Anderson localization of light can be achieved in the deep subwavelength regime.

The behavior of a more complex system of particles can be modeled in more detail by solving Maxwell's equation and obtaining the local-field variation. Owing to the localization mechanism discussed above and subwavelength size and separation of the particles, retardation of electromagnetic waves can be neglected, and Maxwell's equations can be solved in the quasistatic limits. By separating the incident field (E_0) from the depolarization field (E_d) and using continuity of the current [$\nabla \cdot (\epsilon E) = 0$], the depolarization potential ϕ_d in the quasistatic limit can be written as

$$\nabla \cdot (\nabla \epsilon \phi_d) = \nabla \cdot (\epsilon E_0), \tag{7}$$

where $E_d = -\nabla \phi_d$ and ϵ describes the spatial distribution of permittivity inside the composite structure. Equation (7) can be assumed as a system of linear equations $H\phi_d = Q$, where H is the depolarization Hamiltonian (DH) acting on the depolarization potential and Q can be considered as the externally induced charge [29]. This depolarization Hamiltonian can be discretized to take the form of a tight-binding Hamiltonian for noninteracting electrons,

$$H = \sum_i e_i |i\rangle\langle i| + \sum_{i \neq j} t_{ij} |i\rangle\langle j|, \tag{8}$$

where e_i is the potential at site i and t_{ij} represents hopping between sites i and j [29,30]. By selecting the 0.5-nm mesh size, our calculation only addresses classical effects, not, for example, changes in permittivity owing to interface-induced charges in electronic structures.

For random spatial distribution of a composite structure, Eq. (8) is mathematically equivalent to the AH in the presence of a random vector potential [31,32]. This implies localized states as originally predicted by Anderson for random site potentials and by later researchers for random vector potentials (randomness in t_{ij} hopping) where delocalized states are predicted to coexist [32,33]. In the case of DH, t_{ij} corresponds to material permittivity between sites i and j, and e_i is the summation of the materials permittivity between site i and its nearest neighbors ($e_i = -\sum_{j=NN} t_{ij}$). Therefore, we expect eigenstates of a randomly distributed composite material to behave similarly to eigenstates of AH in the presence of a random vector potential, i.e., both localized and delocalized states should exist.

It is also beneficial to note that e_i and t_{ij} are correlated in DH, which takes a different form of randomness compared to AH. However, we should not expect this correlation to cause any difference in the occurrence of localized and delocalized states. Figure 3 compares the localization length of a periodic and random 1D array of granular media. In the case of a periodic array, 10-nm grains ($\epsilon_r = -1$) are separated by 10-nm grain boundaries ($\epsilon_r = 1$). According to Fig. 3(a), most of the eigenstates are delocalized, and the few localized modes correspond to the boundary modes. In Fig. 3(b), we apply 3% randomness to the size of the grains without changing their locations. In this case, as we expected, most of the eigenstates are localized. As discussed in Ref. [29], the role of the delocalized states can be neglected for the case of large systems or a localized incident beam.

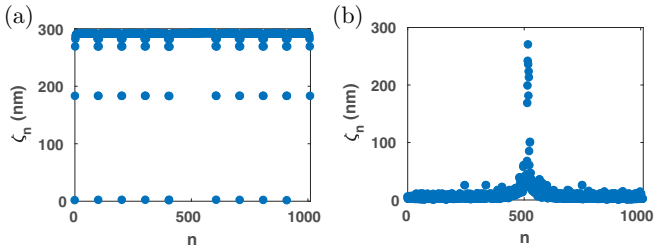

FIG. 3. (a) Localization length of a 1D periodic array of 10-nm grain ($\epsilon_r = -1$) separated by 10-nm grain boundaries ($\epsilon_r = 1$). The length of the array is 500 nm, and a Dirichlet boundary condition is used and (b) localization length of the same array as (a) when 3% variation is added to the size of the grains.

In order to quantify the localization noise, we introduce the parameter $\rho(r)$ as a weighted local density of localized states in the following form:

$$\rho(\vec{r}) = \sum_n \left| \frac{\nabla \psi_n}{\lambda_n} \right|^2, \tag{9}$$

where ψ_n and λ_n are the nth eigenfunction and eigenvalue of DH, respectively. $\rho(\vec{r})$ can be understood as the summation of the depolarization field intensity of different eigenmodes where the depolarization field of each mode is $E_d^n = -\nabla \psi_n / \lambda_n$. Using this definition, the behavior of the local field can be understood in terms of $\rho(\vec{r})$, and spatial fluctuation in $\rho(\vec{r})$ can be considered as a source of localization noise in subwavelength plasmonic devices.

In order to develop a comprehensive framework, we study the fluctuation of $\rho(\vec{r})$ (localization noise) on the performance of HAMR. In HAMR, plasmonic near-field transducers (NFTs) have been used for focusing light on the recording media and increasing its temperature [Fig. 4(a)]. By controlling the temperature, the coercivity of magnetically hard recording grains can be controlled and an $\sim 5\times$ increase in the areal density of hard disk drives can be achieved. In HAMR, each bit of information is usually stored on a cluster of ~ 10 metallic grains ($\sim$5-nm FePt) that are separated by $\sim$1-nm grain boundaries. As a result, the optical beam generated by the NFT should have a diameter smaller than 40 nm. The accuracy of this recording process greatly depends on the grain's temperature: A 3% variation in the recording temperature can significantly decrease the signal-to-noise ratio of the system. Despite the high sensitivity of the device and the potential for randomness of local fields at the deep subwavelength regime, impacts of the local-field variation inside the recording media have been

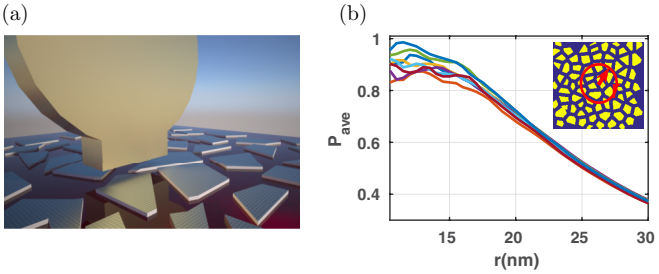

FIG. 4. (a) Schematic of a lollipop NFT and (b) normalized average absorption power per volume of FePt of eight different recording media as a function of observation window radius. The average size of the FePt grains is assumed to be 9 nm separated by 1-nm SiO_2 grain boundaries. The recording layer is located atop an 8-nm MgO seed layer and a 60-nm gold heat sink. The distance between the NFT and the recording media is also assumed to be 8 nm.

neglected in most studies by utilizing effective medium theory [34,35].

In Fig. 5, $\rho(\vec{r})$ is compared with a FDTD [36] simulation in an arbitrary realization of HAMR media. For the FDTD simulation, we use the total field scatter field method to locally shine a circular polarized plane wave on the recording media: It excites all local modes. For calculating $\rho(\vec{r})$, a two-dimensional (2D) version of the depolarization Hamiltonian is evaluated based on the general approach for calculating the 2D Kirchhoff Hamiltonian [29]. According to Fig. 5, there is good agreement between the $\rho(\vec{r})$ and the FDTD simulation. Therefore, topography of $\rho(\vec{r})$ can be used for engineering of the HAMR media.

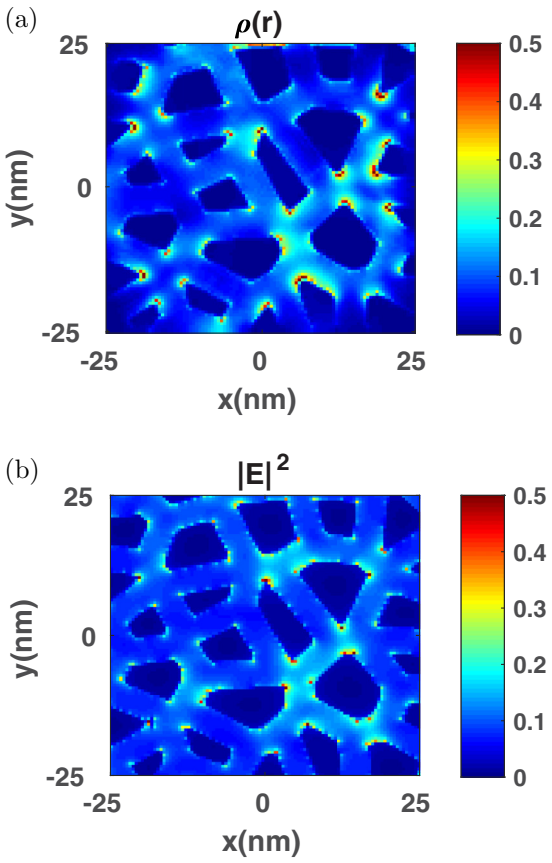

FIG. 5. (a) Weighted density of state of the localized modes inside HAMR media containing FePt ($n = 3.3 + 4.3i$) grains separated by 4-nm SiO_2 ($n = 1.5$) grain boundaries and (b) field intensity inside the same media as (a) calculated by the finite difference time-domain (FDTD) method.

As depicted in Fig. 5, the location of the hot spots cannot be explained from the perspective of individual particle geometry. For an isolated particle, we expect to observe enhancement in the electric field at sharp corners owing to the lightening rod effect. However, according to Fig. 5, particles with similar shapes and sizes respond differently to the incident optical beam: Sharp corners with similar angles cause different field enhancements, the intensity of the electric field is different around particles with similar geometry, and there is no consistent size dependency in the field enhancement. These observations suggest that Anderson localization is the dominant field enhancement mechanism in an ensemble of plasmonic particles and that studying geometry of isolated particles can lead to misleading results.

Consequences of these localized modes in the HAMR performance can be demonstrated more clearly by calculating the average absorption power as a function of the observation window for different realizations of granular recording media. For this purpose, we calculate absorption power per unit volume of FePt for eight different recording media in a circular observation window with the radius located below the lollipop NFT [34]. According to Fig. 4, for a large observation window, the effects of randomness of the localized depolarization modes are averaged out. However, for $r < 25$ nm, which is in the operating length scale of HAMR, randomness in the localized mode can add a significant variation in the absorption power. This variation in the absorption power leads to variation in the temperature of the recording media, which is usually considered to be the main source of noise in HAMR but is typically attributed to much different (nonoptical) sources.

In conclusion, we show that enhancement of the depolarization field, and thus energy absorption, of metallic particles greatly depends on their shapes. This shape dependency can lead to Anderson localization of light in the deep subwavelength regime. In the case of randomly distributed clusters of particles, we show that the electrostatic Hamiltonian maps onto the Anderson Hamiltonian for electrons in the presence of a random vector potential, and the localized mode of the depolarization field is responsible for the randomness in the local field. We also demonstrate that optical nanodevices, such as HAMR, that operate on a length scale that is comparable to these localized modes, will experience a localization noise that can significantly affect their scalability.

The authors acknowledge funding from Western Digital Corporation. A.G. acknowledges a Doctoral Dissertation Fellowship from the University of Minnesota. The authors also acknowledge the Minnesota Supercomputing Institute (MSI) at the University of Minnesota for providing resources that contributed to the research results reported within this paper (see Ref. [37]).

[1] S. John, Phys. Rev. Lett. **53**, 2169 (1984).

[2] H. De Raedt, A. Lagendijk, and P. de Vries, Phys. Rev. Lett. **62**, 47 (1989).

[3] D. S. Wiersma, P. Bartolini, A. Lagendijk, and R. Righini, Nature (London) **390**, 671 (1997).

[4] A. Chabanov, M. Stoytchev, and A. Genack, Nature (London) **404**, 850 (2000).

[5] T. Schwartz, G. Bartal, S. Fishman, and M. Segev, Nature (London) **446**, 52 (2007).

[6] L. Levi, Y. Krivolapov, S. Fishman, and M. Segev, Nat. Phys. **8**, 912 (2012).

[7] F. Rüting, P. Huidobro, and F. García-Vidal, Opt. Lett. **36**, 4341 (2011).

[8] X. Shi, X. Chen, B. A. Malomed, N. C. Panoiu, and F. Ye, Phys. Rev. B **89**, 195428 (2014).

[9] S. Pandey, B. Gupta, S. Mujumdar, and A. Nahata, Light: Sci. Appl. **6**, e16232 (2017).

[10] S. A. Maier and H. A. Atwater, J. Appl. Phys. **98**, 011101 (2005).

[11] S. Lal, S. Link, and N. J. Halas, Nat. Photonics **1**, 641 (2007).

[12] J. A. Schuller, E. S. Barnard, W. Cai, Y. C. Jun, J. S. White, and M. L. Brongersma, Nature Mater. **9**, 193 (2010).

[13] H. A. Atwater and A. Polman, Nature Mater. **9**, 205 (2010).

[14] M. I. Stockman, Opt. Express **19**, 22029 (2011).

[15] E. Fort and S. Grésillon, J. Phys. D: Appl. Phys. **41**, 013001 (2007).

[16] X. Li and M. I. Stockman, Phys. Rev. B **77**, 195109 (2008).

[17] A. K. Sarychev and V. M. Shalaev, Phys. Rep. **335**, 275 (2000).

[18] P. A. Lee and T. Ramakrishnan, Rev. Mod. Phys. **57**, 287 (1985).

[19] Kramer, Rep. Prog. Phys. **56**, 1469 (1993).

[20] I. M. Lifshits, S. A. Gredeskul, and L. A. Pastur, *Introduction to the Theory of Disordered Systems* (Wiley-Interscience, New York, 1988).

[21] M. H. Kryder, E. C. Gage, T. W. McDaniel, W. A. Challener, R. E. Rottmayer, G. Ju, Y.-T. Hsia, and M. F. Erden, Proc. IEEE **96**, 1810 (2008).

[22] L. Pan and D. B. Bogy, Nat. Photonics **3**, 189 (2009).

[23] R. E. Rottmayer, S. Batra, D. Buechel, W. A. Challener, J. Hohlfeld, Y. Kubota, L. Li, B. Lu, C. Mihalcea, K. Mountfield *et al.*, IEEE Trans. Magn. **42**, 2417 (2006).

[24] C. F. Bohren and D. R. Huffman, *Absorption and Scattering of Light by Small Particles* (Wiley, Hoboken, NJ, 2008).

[25] W.-H. Yang, G. C. Schatz, and R. P. Van Duyne, J. Chem. Phys. **103**, 869 (1995).

[26] S.-O. Guillaume, F. J. García de Abajo, and L. Henrard, Phys. Rev. B **88**, 245439 (2013).

[27] L. Zhao, K. L. Kelly, and G. C. Schatz, J. Phys. Chem. B **107**, 7343 (2003).

[28] D. Citrin, Nano Lett. **5**, 985 (2005).

[29] A. K. Sarychev and V. M. Shalaev, *Electrodynamics of Metamaterials* (World Scientific, Singapore, 2007).

[30] S. Grésillon, L. Aigouy, A. C. Boccara, J. C. Rivoal, X. Quelin, C. Desmarest, P. Gadenne, V. A. Shubin, A. K. Sarychev, and V. M. Shalaev, Phys. Rev. Lett. **82**, 4520 (1999).

[31] N. Hatano and D. R. Nelson, Phys. Rev. Lett. **77**, 570 (1996).

[32] D. N. Sheng and Z. Y. Weng, Phys. Rev. Lett. **75**, 2388 (1995).

[33] A. Eilmes, R. A. Römer, and M. Schreiber, Eur. Phys. J. B **1**, 29 (1998).

[34] W. Challener, C. Peng, A. Itagi, D. Karns, W. Peng, Y. Peng, X. Yang, X. Zhu, N. Gokemeijer, Y.-T. Hsia *et al.*, Nat. Photonics **3**, 220 (2009).

[35] B. C. Stipe, T. C. Strand, C. C. Poon, H. Balamane, T. D. Boone, J. A. Katine, J.-L. Li, V. Rawat, H. Nemoto, A. Hirotsune *et al.*, Nat. Photonics **4**, 484 (2010).

[36] Lumerical Solutions, Inc., http://www.lumerical.com/tcad-products/fdtd/

[37] http://www.msi.umn.edu